

## **Modelling and Experimental Results of a 26GHz Integrated Passively Modelocked Ring Laser.**

Y. Barbarin<sup>1</sup>, E.A.J.M Bente<sup>1</sup>, M.J.R. Heck<sup>1</sup>, D. Lenstra<sup>1</sup>, J.H. den Besten<sup>1</sup>,  
M.K. Smit<sup>1</sup> and J.J.M. Binsma<sup>2</sup>

<sup>1</sup>) COBRA Research Institute, Technische Universiteit Eindhoven,  
Postbus 513, 5600 MB Eindhoven, The Netherlands.

<sup>2</sup>) JDS Uniphase, Prof. Holstlaan 4, NL-5656 AA, Eindhoven, The Netherlands

*A model of an integrated modelocked ring laser is presented. This model is used to analyse the behaviour of a 26GHz mode-locked ring laser fabricated with active-passive integration. The semiconductor amplifier and the saturable absorber are described using rate equations. The bandwidth limitation is simulated by a digital filter. The laser is modelled by segmenting the ring in parts. This allows the inclusion of intra-cavity reflections in the model. Self-starting, self-pulsating and modelocking operation have been simulated in a bi-directional mode. Our experimental and theoretical results are compared and discussed.*

### **Introduction**

Modelocked lasers are key components for high bit rate telecommunication. Optical Time Domain Multiplexing (OTDM) is a solution to increase the rate of a WDM channel up to 160 Gbit/s or higher. The application of OTDM requires clock recovery and clock division for demultiplexing the signals. In our project we are developing an All Optical Clock Recovery (AOCR) device based on an injection seeded passively ModeLocked Laser (MLL). For this application the ring configuration has two advantages. Firstly, the repetition rate of the laser is controlled accurately by photolithography as opposed to a device with cleaved facet mirrors. Secondly the ring laser configuration is more suitable for the injection seeding process that is at the centre of the AOCR. The butt-joint active-passive integration technology we have used makes the laser design suitable for further integration with other devices such as an all-optical switch. In this paper we present simulations and first experimental results of such device.

### **Modelocked laser device**

The device we want to analyse with our model has been realised in the InP/InGaAsP material system with active-passive integration. A picture of the fabricated device is given in figure 1; waveguides are visible as dark lines. Light is coupled out from the ring cavity using a Multi-Mode Interferometer (MMI). To better understand the design, one must realise that the positions and sizes of the active regions were predetermined through the re-growth process. Two bulk Semiconductor Optical Amplifier (SOA) are used. The amplifier is 500  $\mu\text{m}$  long. To realise a 30 $\mu\text{m}$  saturable absorber a waveguide was positioned to cross the second active area at an angle. For this design, the ring laser Free Spectral Range (FSR) could not be over 26 GHz.

To reduce the intra-cavity loss and to realise bends with a 100 $\mu$ m radius of curvature, deep and shallow waveguide were combined. To reduce facet reflectivity, output waveguides (not visible in the figure 1) are angled by 7 $^\circ$  with respect to the facets normal and contains mode filters [1].

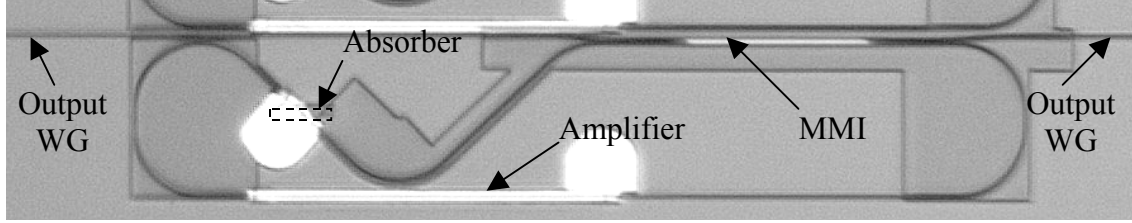


Fig.1 Optical microscope image of a part of the fabricated chip with a 26GHz

## Modelling

To simulate our device, a numerical bi-directional model has been developed. The amplifier and the absorber are described using rate equations. The ring is divided into segments that are equal in optical length (Fig.2). Every 25fs the photon densities (CW and CCW) and carrier densities are calculated for all segments. Then the photon densities are transferred to the next segments and the carrier density values are saved in active segments for the next step. A digital Bessel filter (14<sup>th</sup> order) simulates the gain bandwidth limitation. The filter transmission spectrum is close to the measured gain spectrum (fig.3) and it is numerically stable. Small reflections ( $2 \cdot 10^{-4}$ ) at the different active passive butt-joints interfaces [2] and at the MMI inputs [3] are introduced.

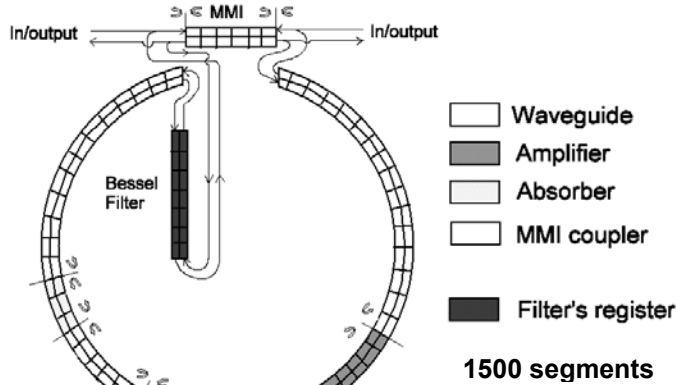


Fig.2 Structure of the MLL modelled.

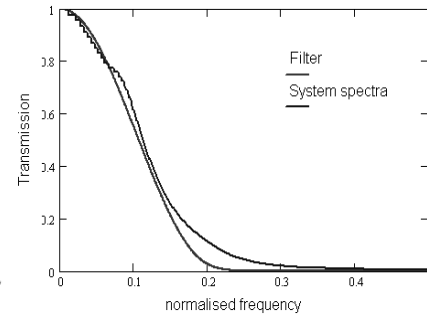


Fig.3 Spectra of the amplifier and transmission of the digital Bessel filter.

The SOA is described using the standard rate equations and the logarithmic gain-current density validated in [4].

$$\frac{\delta\phi^{CW,CCW}(x,t)}{dt} = \phi^{CW}(x,t) \cdot \left[ \alpha_{amp} \cdot N0 \cdot \ln\left(\frac{N(x,t)}{N0}\right) \cdot Vg \cdot \Gamma - \frac{Loss_{seg}(N(x,t))}{\tau_{seg}} \right] + B \cdot \Gamma \cdot N(x,t)^2 \cdot \beta$$

$$\frac{\delta N(x,t)}{dt} = - \left[ \phi^{CW}(x,t) + \phi^{CCW}(x,t) \right] \cdot \alpha_{amp} \cdot N0 \cdot \ln\left(\frac{N(x,t)}{N0}\right) \cdot Vg - \frac{N}{\tau_{car.Amp}} - B \cdot N(x,t)^2 - C \cdot N(x,t)^3 + W(t)$$

Here  $\phi^{CW,CCW}$  are the clock wise and counter clock wise photon densities,  $N$  is the active region carrier density,  $W(t)$  is the carrier density generated in the active layer by the

injection current,  $N_0$  is the carrier transparency density,  $V_g$  is the group velocity,  $\alpha_{amp}$  is the linear gain coefficient,  $\tau_{car,amp}$  is the carrier lifetime,  $B$  is the bimolecular recombination coefficient,  $C$  is the Auger recombination coefficient,  $\Gamma$  is the confinement factor,  $Loss_{seg}$  are the sum of the different losses for one segment (the scattering loss, the free carrier loss in the cladding, and the free carrier absorption within the active layer which depends of the carrier density),  $\tau_{seg}$  is the time segment and  $\beta$  is the spontaneous emission coupling factor.

The absorber is a short SOA that is reverse biased, it is described with similar rate equations as the amplifier without carrier injection. The carrier lifetime of the absorber depends of the reverse bias applied, but the relation has not been implemented.

### Simulation and experimental results

Using this model, we have calculated the performance of the modelocked ring laser shown in figure 2. The laser operates in both directions. A simulation of the self-starting is plotted in figure 4. The laser start with relaxation oscillations and modelocking sets in more slowly. A steady mode-locked state is reached after 16ns (450 roundtrips). In this laser, the CW and CCW pulses meet in the amplifier and not in the absorber. If the pulses enter and leave the amplifier at the same time, it optimises the amplifier recovery time. Both pulses will have the same gain. Then in the first half of the amplifier, pulses are amplified, but after meeting in the centre, the amplifier is saturated by the oncoming pulse. This reduces the trailing edge of the pulses and thus strengthens the modelocking mechanism. The absorber is located at a quarter roundtrip time from the centre of the amplifier, which means a pulse will pass through it every half roundtrip time (17ps).

Self-starting, self-pulsating and modelocking operation did show up in the simulations. The different regimes of operation are plotted in the figure 5. Self-pulsation is indicated in black. The real device did not show this behaviour and was very sensitive to changes in temperature and current. Windows of working operation become very small. We suspect that continuous small changes in the temperature distribution in the device cause a variation in the optical path length, which prevents stable operation. In the simulations modelocking operation with pulse widths below 1ps were shown for an absorber carrier lifetime lower than 25ps. Such a pulse length performance has been observed intermittently close to the maximum current and reverse-bias voltage. Measured and simulated autocorrelation traces are plotted in figure 6. The second measured pulse is not completely visible due to a limit of the autocorrelator. Stable operation has been measured with 5 pulses in the cavity. The measured RF spectrum from a 50GHz photodiode is shown in figure 7. The peak at the FSR frequency is 40dB over the noise floor and has a width of less than 1MHz. This demonstrates stable

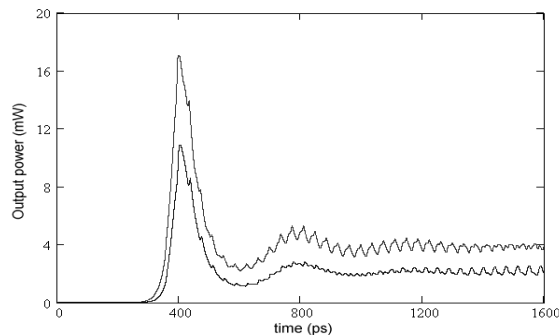


Fig.4: Simulated self-starting  $I=140$  mA  $T_{car}=20$ ps

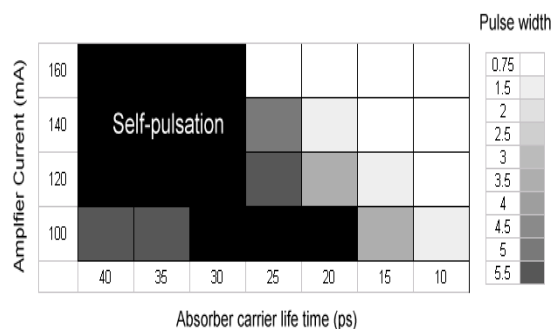


Fig.5: Simulated regimes of operation of the RMLL

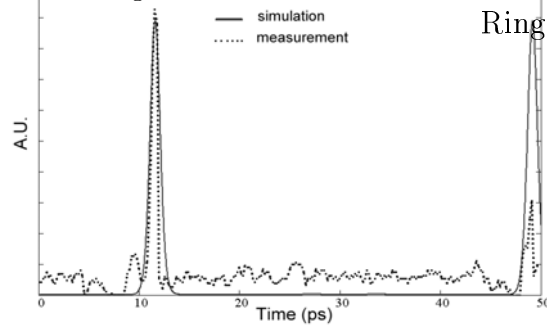


Fig. 6: Simulated autocorrelation trace  $I=160mA$   $T_{car}=15ps$   
 Measured autocorrelation trace  $I=169mA$   $V=-2.1V$

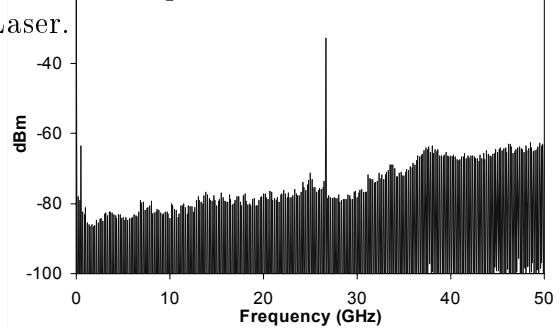


Fig. 7: Measured RF-spectrum  $I = 167.5mA$   $V = -2.0V$

modelocking. In our opinion, the five pulses are generated by the intra-cavity reflections from the left butt-joint of the amplifier and the upper butt-joint of the absorber, which is one fifth of the cavity roundtrip time. We have attempted to implement this regime in our model. We have found a similar mode that is stable for 3ns (80 roundtrips) but then one of the pulses becomes dominant and suppresses the others. For currents higher than 120mA and carrier lifetime longer than 30 ps, simulations show slow modulations at around 350MHz resulting from competition between the CW and the CCW pulses. Those modulations have been observed in the RF spectrum of the real device.

## Conclusion

We have presented a model of an integrated modelocked ring laser. The model has been used to analyse the behaviour of a 26GHz mode-locked ring laser fabricated with active-passive integration. Experiment results show that intra-cavity reflections make it very difficult to obtain a stable modelocked state. In small windows of operation, CW, modelocked and self-pulsating regimes have been observed. Similar regime have been observed in the model. This model will be used to design new mode-locked lasers with reduced intra-cavity reflections.

## Acknowledgment

This research is supported by -the Towards Freeband Communication Impulse of the technology programme of the Ministry of Economic Affairs of the Netherlands.

## Reference

- [1] J. Leuthold, R. Hess, J. Eckner, P. A. Besse, and H. Melchior "Spatial mode filters realized with multimode interference couplers", *Opt. Lett.* 21, 1996, pp 836-838
- [2] Y. Barbarin, E.A.J.M Bente, C. Marquet, E.J.S Leclère, M.K. Smit and J.J.M. Binsma "Measurements of Reflectivities on Butt-Joint Active-Passive Interfaces in Extended Cavity Fabry-Pérot Lasers" in *Proc. IEEE/LEOS Benelux Chap.* (2004)
- [3] D. Erasme, L.H. Spiekman, C.G.P. Herben, M.K. Smit, and F.H. Groen, "Experimental assessment of the reflection of passive multimode interference couplers" *IEEE Photon. Technol. Lett.*, vol. 9, no. 12, Dec. 1997, pp. 1604-1606
- [4] T.A. DeTemple, C.M. Herzinger, " On the semiconductor laser logarithmic gain-current density relation" *IEEE J.Q.E.* vol 39. 1933 pp 1246-1252